Machinery & Energetics
Vol. 14, No. 2. 2023

Journal homepage:
https://technicalscience.com.ua/en

UDC 621.313.33:621.318.122
DOI: 10.31548/machinery/2.2023.09

Krzysztof Mudryk
Professor
University of Agriculture in Krakow
30-149, 21 Adam Mitskevich Ave., Krakow, Poland
https://orcid.org/0000-0002-6212-6958

Taras Hutsol
Professor
University of Agriculture in Krakow
30-149, 21 Adam Mitskevich Ave., Krakow, Poland
https://orcid.org/0000-0002-9086-3672

Nikolay Zablodskiy*
Doctor of Technical Sciences, Professor
National University of Life and Environmental Sciences of Ukraine
03041, 15 Heroiv Oborony Str., Kyiv, Ukraine
https://orcid.org/0000-0001-8889-8158

Dmytro Sorokin
PhD in Technical Sciences, Associate Professor
National University of Life and Environmental Sciences of Ukraine
03041, 15 Heroiv Oborony Str., Kyiv, Ukraine
https://orcid.org/0000-0002-1762-9724

Serhii Usenko
PhD in Technical Sciences, Associate Professor
National University of Life and Environmental Sciences of Ukraine
03041, 15 Heroiv Oborony Str., Kyiv, Ukraine
https://orcid.org/0000-0001-7225-9589

A study of electrothermomechanical converter for technological purposes with nonlinear changes in the loading and cooling medium

Abstract. Heavy temperature processes with high-temperature loads require optimisation of technological processes, ensuring high reliability and combining rotating parts of electric machines with actuators to achieve greater efficiency of electromechanical converters. The research aims to provide a theoretical justification and experimental confirmation of the effect of higher harmonics in the air gap under nonlinear changes in the temperature of the medium. The research is based on the basic principles of electrodynamics, heat and mass transfer, mathematical modelling by the finite element method, and experimental verification of multi-physical parameters. Based on the analysis of the differential equation for determining the increase in the surface temperature of a ferromagnetic rotor under conditions of nonlinear temperature changes in the environment surrounding the electromechanical converter, the regularities of the formation of the free and forced components of the instantaneous temperature values of the massive rotor are established. Depending

Article's History: Received: 18/01/2023; Revised: 22/03/2023; Accepted: 26/04/2023.

Suggested Citation:
Mudryk, K., Hutsol, T., Zablodskiy, N., Sorokin, D., & Usenko, S. (2023). A study of electrothermomechanical converter for technological purposes with nonlinear changes in the loading and cooling medium. *Machinery & Energetics,* 14(2), 9-22. doi: 10.31548/machinery/2.2023.09.

*Corresponding author

on the mode of interaction between the load-cooling medium and the electromechanical part of the screw units, kinematic diagrams of single-mass and two-mass systems with variable or constant moments of inertia and stiffness were formed. According to the size of the electromagnetic system of the experimental sample, a mathematical model for studying thermal and electromagnetic processes was built. The regularities of the spatial distribution of the temperature of the screw electromechanical unit are determined. The spectra of higher harmonics of voltage and current in the frequency range from 0 to 50 kHz have been experimentally determined, which confirms the presence of the effect of generating higher harmonics when the temperature of the medium surrounding the rotor screw changes. The detected harmonic spectrum affects both the formation of the dynamics of the rotating system and additional thermal power while increasing the overall efficiency of the screw electromechanical converter. The practical value of the obtained results lies in the possibility of predicting the optimal indicators of interrelated electromagnetic and heat exchange processes in screw electromechanical converters for technological purposes

Keywords: higher harmonics spectrum; ferromagnetic hollow rotor; biomass; temperature field; electromagnetic field; design; and technological scheme

INTRODUCTION

Applications of electromechanical transducers exist for which, in addition to the concept of efficiency, reliable operation in a process environment with high temperature, pressure and humidity or a limited volume is also a significant parameter. To predict losses, A. Laidoudi *et al.* (2020) proposed an analytical model that is combined with a thermal model to predict the temperature in different parts of the machine, its impact on the parameters that are important for the performance of an electric machine (EM) at high temperatures.

The issue of finding alternative solutions to replace organic insulating materials that cannot withstand hot operating conditions is relevant. In the studies of M. Lefik *et al.* (2019), H. Elmadah *et al.* (2019), E.N. Juszczak *et al.* (2020) performed a comparative analysis of the laminated and solid rotor of a synchronous machine operating at high temperatures using windings made of inorganic materials. The study also presents the application of three-dimensional combined electromagnetic and thermal analysis of new machine designs designed for elevated temperatures.

A wide range of technological processes with heavy temperature loads exists that requires the direct connection of rotating EM parts with actuators. M.M. Mazlan *et al.* (2019), and F. Campuzano *et al.* (2019) proved the effectiveness of using a screw converter, which is attractive due to its versatility in processing various types of materials, regardless of the pace of the technological process. The influence of hydrolysis parameters on the mixing torque was investigated for single- and twin-screw electromechanical converters by P. Singha & K. Muthukumarappan (2016) and C. Feng *et al.* (2019). In these studies, regression models were developed to establish the correlation between system parameters and time-varying parameters. The results showed that increasing the processing temperature beyond the recommended levels led to a decrease in the viscosity of the raw material, the pressure in the processing medium, and the specific mechanical energy. In addition, M. Mushtruk *et al.* (2020) investigated the issue of high energy consumption associated with machining in an electromechanical screw converter. In the study, mathematical modelling was carried out and the power and energy parameters of the technical system were determined.

V. Gritsyuk *et al.* (2022) noted that 3D printing technologies for large-scale structures allow architects and builders to significantly expand the boundaries of building design and increase the efficiency of their construction. Mobile robotic platforms for 3D printing are increasingly being introduced in the construction industry, as well as in the production of road surfaces, which helps to solve the problem of limited working space. The typical design of the extruder unit of a robotic platform for 3D printing large-scale structures can be improved by combining an electric motor, a screw extruder, and a heater in one housing. The proposed screw electro-thermomechanical converter uses an external screw rotor that simultaneously performs the functions of an induction motor rotor, heating element, actuator, and protective casing. For converters operating under harsh conditions, the use of field calculation methods is relevant.

As such, along with solving the problem of ensuring the reliability of electromechanical converters in harsh environments, a scientific demand for improving the energy efficiency of their use through structural, functional, and thermal integration with the technological environment is present.

The research aims to theoretically substantiate and experimentally confirm the effect of the appearance of higher harmonics in the air gap under nonlinear changes in the temperature of the medium surrounding the electromechanical converter in screw technological systems.

MATERIALS AND METHODS

The research was carried out at the Department of Electrical Engineering, Electromechanics and Electrical Technologies of the National University of Life and Environmental Sciences of Ukraine in 2020-2022. The study considered two modifications of an electromechanical converter for technological purposes, in which the processed raw material acts as a loading and cooling medium: in a twin-screw electromechanical hydrolyser; use of an electric screw unit for grinding and pyrolysis of plant waste biomass. In this

case, the actuator (auger) is combined with the outer rotor of the electromechanical converter. The electromechanical converter was presented as a six-pole (Fig. 1) with an electrical circuit characterised by voltage U and frequency f, a mechanical circuit defined by torque M and mechanical rotational speed n, and a thermal circuit characterised by heat quantity Q and temperature T.

The design and technological scheme of a twin-screw electromechanical hydrolyser for the production of feed protein meal is shown in Figure 2.

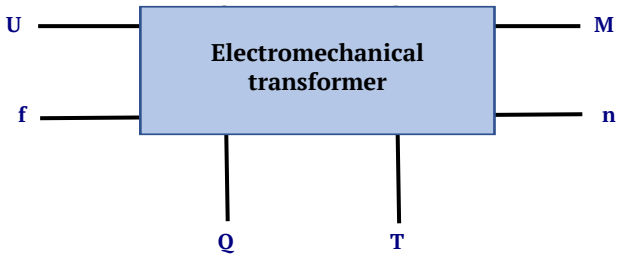

Figure 1. Hexagon-pole electromechanical converter
Source: compiled by the authors

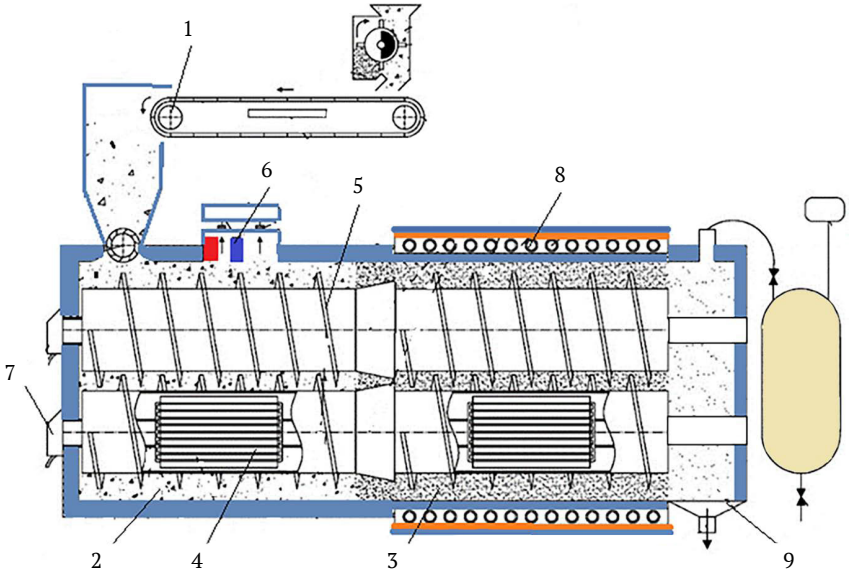

Figure 2. Design and technological scheme of a twin-screw electromechanical hydrolyser
Note: 1 – loading device with magnetic and electrodynamic separators; 2, 3 – sealing and reaction working zones; 4 – cylindrical inductors of a rotating magnetic field; 5 – rotor screw; 6 – magnetic deaeration chamber for raw materials; 7 – power supply cable connection boxes; 8 – induction heating device with thermal insulation and electromagnetic shield; 9 – vacuum-pulse product unloading device
Source: compiled by the authors based on (Patent of Ukraine No. 125774, 2022)

The feather and fluff raw material with an initial moisture content of 60-80 % was supplied to the feeding device of the screw unit, where it was exposed to electromagnetic fields to remove metal particles and the water-air component was removed from the raw material to the level of residual moisture (35-45 %) using a belt vacuum filter. In the first working area of the screws, a raw material seal (plugs) was created by reducing the flow section of the screw unit and providing a pressure of 1 MPa to 20 MPa. Along with the compaction, the feedstock was heated to a temperature of 60°C, exposed to a gradient magnetic field with a frequency of 1-50 Hz and an induction of 0.025T, and magnetic deaeration was performed. The raw material was then fed into the reaction working area of the screws, where it was loosened by the reduced diameter part of the screw turns, mixed and crushed at a temperature of 180-260°C to obtain a crushed mass. At the same time, a gradient magnetic field with a frequency of 1-50 Hz and an induction of 0.065 T was applied in this area of the installation and four-sided heat energy was supplied to the layer of down and feather raw materials. In the vacuum-pulse device, a vacuum effect was applied every 10-60 s to obtain a product with a moisture content of 8-12%. The design and technological scheme are shown in Figure 3.

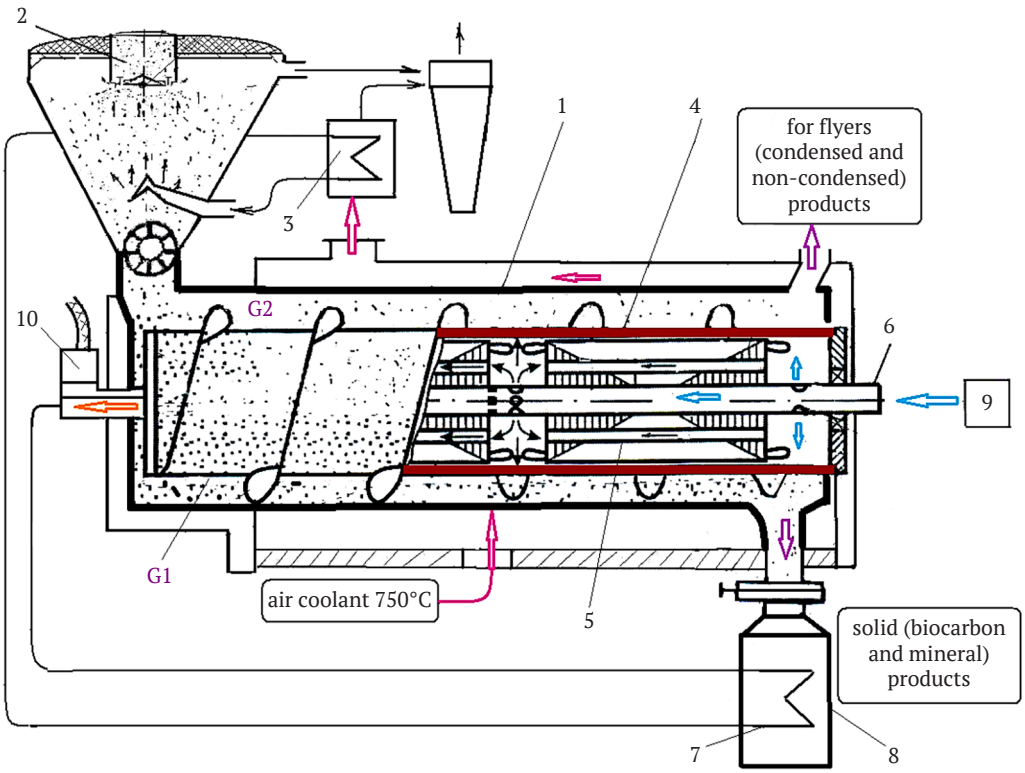

Figure 3. Design and technological scheme of the plant biomass pyrolysis unit
Note: 1 – pyrolysis chamber; 2 – hopper with loading devices; 3 – heat recovery system; 4 – rotor screw; 5 – cylindrical inductors of a rotating magnetic field; 6 – fixed hollow shaft; 7 – heat exchanger; 8 – solid product unloading chamber; 9 – air supply system; 10 – power supply cable connection box
Source: compiled by the authors based on (Zablodskiy *et al.*, 2020)

The process gas with an excess air ratio of less than one was burned in the process furnace to produce a high-temperature (750°C) gas coolant, which was supplied for external heating of the pyrolysis chamber1. The finely fractionated biomass was supplied in portions through a lid with a magnetic closure to the hopper of loading device 2, where it was pre-dried and heated (Zablodskiy *et al.*, 2020). Using the feeder, the biomass was fed into the screw-type sealed pyrolysis chamber 1, where the biomass layer was heated on the one hand through the chamber walls by the coolant generated during the combustion of fuel in the process furnace, and on the other hand by conductive heat transfer and radiation from the surface of the outer massive rotor 4 of the electromechanical converter connected to a three-phase power supply network.

In both modifications under consideration, the mechanical energy of rotation of the rotor-auger was created by the interaction of a rotating magnetic field and eddy currents in the ferromagnetic array of the rotor-auger. The working load-cooling medium was in direct contact with the rotor-auger. Depending on the loading mode, the kinematic diagram of the mechanical part of the screw units can be presented in the following forms:

- single-mass system at idle (Fig. 4a);
- two-mass system operating with variable stiffness C_{12} and variable moment of inertia J_2 of the viscous mass in the mode of gradual filling of the screw (Fig. 4b);
- two-mass system with constants C_{12} and J_2 in the basic mode of operation (Fig. 4c);
- two-mass system with constants C_{12} and J_2 in the screw release mode (Fig. 4d);

The stiffness coefficient C_{12} contains two components related to the ratio of elastic bond load and rotational and translational deformation.

During rotation, the areas of the outer surface of the screw rotor periodically fall into different temperature zones above and below the shaft axis (Fig. 3). A similar picture is observed in the working areas of a twin-screw electromechanical hydrolyser (Fig. 2) in the layers of raw materials located between the screw rotors and the walls of the sealing and reaction working areas, as well as between the screw surfaces. Since the rotor rotation frequency is almost constant at a certain screw capacity, it is possible to observe the process of periodic changes in the temperature of the medium washing the outer surface of the ferromagnetic rotor.

In the first approximation, it was assumed that the temperature increase of the medium ΔT_{en} varied periodically (sinusoidally) in time. The differential equation for determining the temperature increase of the surface of a ferromagnetic rotor will be as follows:

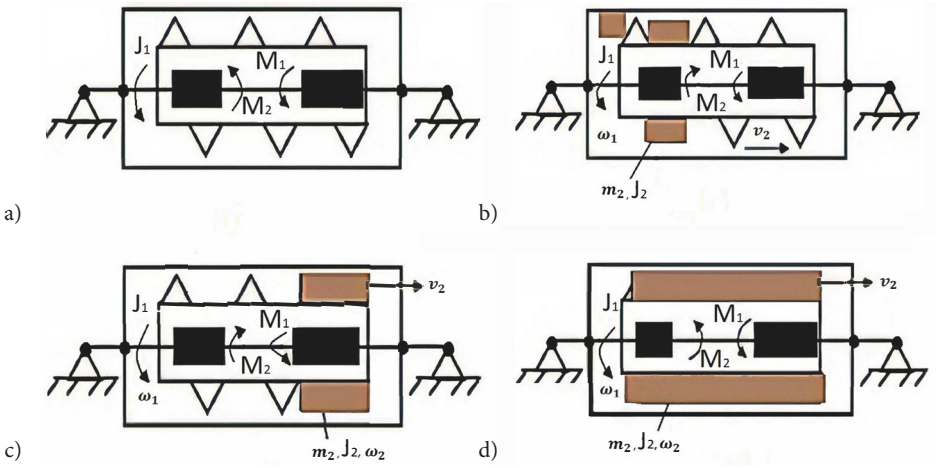

Figure 4. Kinematic diagrams of screw units

Note: J_1 – a moment of rotor screw inertia; J_2 – a moment of viscous mass inertia; M_1, M_2 – rotation under motion and braking modules; υ_2 – viscous mass velocity; m_2 – the weight of the substance loaded into the screw; ω_1 ,ω_2 – angular velocity of the rotor screw and viscous mass, respectively

Source: compiled by the authors

$$R_r \frac{d(\Delta T_r)}{dt} + \Delta T_r = \Delta T_{en.m}\, sin(\omega_r t), \quad (1)$$

where R_r – thermal time constant of the rotor design zone; $\Delta T_{en.m}$ – environment temperature amplitude increase; ΔT_r– rotor temperature increase; ω_r – cyclic frequency of change in the temperature of the medium, equal to the angular frequency of rotation of the rotor.

Thermal time of ferromagnetic rotor:

$$R_r = \frac{m_r c_r}{2 \cdot G_{TCR}}, \quad (2)$$

where m_r, c_r – respectively mass and specific heat capacity of the rotor material; G_{TCR} – rotor heat conductivity.

Heat conductivity G_{TCR} is calculated for a homogeneous cylindrical wall with heat sources and heat dissipation through the outer wall (Subramanian, 2014):

$$G_{TCR} = \frac{4\pi\lambda \cdot l_r}{\frac{2r_2^2}{r_2^2 - r_1^2} \ell n \frac{r_2}{r_1}}, \quad (3)$$

where l_r – rotor length; r_1, r_2 – inner and outer radii of the cylindrical rotor, respectively; λ – rotor material heat conductivity coefficient.

Formula (3) is valid provided that the depth of penetration of the electromagnetic wave into the rotor Δ_{ew} in the operating sliding mode is approximately equal to the rotor wall thickness $(r_2 - r_1)$.

When $(r_2 - r_1) > \Delta_{ew}$ an exponential heat release function must be included in the calculations $q_{uo} te^{-\beta X/(r_2 - r_1)}$, where q_{vo} – specific heat emission in a thin layer at $x_o \approx R_1$; β – coefficient of uneven loss distribution.

A more accurate result for calculating thermal conductivity G_{TCR} can be obtained by considering the helical blades (fins) of the rotor, which significantly intensify heat transfer between the rotor's inner surface and the environment. In this case, the following calculation formula can be used:

$$G_{TCR} = \frac{2\pi \cdot r_2 \cdot l_r}{\frac{1}{\alpha_1} + \frac{r_2 - r_1}{\lambda} + \frac{1}{\alpha_2[1 + A_{os}(k_{os} - 1)]}}, \quad (4)$$

where α_1 – the heat transfer coefficient on the un-finned surface of the rotor wall; α_2 – is the heat transfer coefficient from the finned rotor surface. The equality of heat transfer coefficients with smooth α_s surface and rib surface α_r; A_{os} – rib efficiency coefficient; k_{os} – the coefficient of finning of the rotor surface, equal to the ratio of the total area of the finned surface to the area of the smooth rotor surface.

Rib efficiency coefficients at height h_r and thickness δ_r, manufactured from material with heat conductivity λ_r:

$$A_{os} = \varepsilon_к \frac{thB}{B}, \quad (5)$$

where $B = h_r[2\alpha_r / \lambda_r \delta_r]^{0,5}$.

The value of the correction factor ε_k is a function of the ratio of the excess temperatures at the end and base of the fin and the ratio of the outer radii of the fin (blade) and the smooth rotor.

The solution to equation (1) is obtained as two components.

Forced component $\Delta T'_r$ can be given as:

$$\Delta T'_r = \Delta T_{en.m} e^{j\omega_r t}. \quad (6)$$

Using the symbolic method of operations with complex numbers, the differential equation (1) can be represented as:

$$R_r \cdot \frac{d(\Delta T_{rm} e^{j\omega_r t})}{dt} + \Delta T_{r.m} e^{j\omega_{rr} t} = \Delta T_{en.m} e^{j\omega_r t}, \quad (7)$$

where ΔT_{rm} – amplitude value of the rotor temperature increase.

Having found the derivative in (7), the amplitude value of the temperature increase of the massive rotor was determined.

$$\Delta T_{rm} = \frac{\Delta T_{en.m}}{1+j\omega_r R_r}. \quad (8)$$

Then, the phase angle φ_r between increases ΔT_r and ΔT_{en} was found:

$$\varphi_r = arctg(-\omega_r R_r), \quad (9)$$

where symbol "–" shows the increase ΔT_r lacking on the increase phase ΔT_{en}.

As a result, the stationary solution of the differential equation (1) concerning the forced component can be represented as follows:

$$\Delta T_r' = \frac{\Delta T_{en.m}}{\sqrt{1+\omega_r^2 R_r^2}} sin(\omega_r t - \varphi_r). \quad (10)$$

To find the free component of the right, the part of equation (1) was set to zero:

$$R_r \cdot \frac{d(\Delta T_r)}{dt} + \Delta T_r = 0. \quad (11)$$

An equation was made:

$$R_r \cdot Z + 1 = 0, \quad (12)$$

where $Z = \frac{d(\Delta T_r)}{dt}$.

Value $Z = -1/R_p$. Then the partial solution was represented as an exponent:

$$\Delta T_r'' = Ae^{-t/R_r}, \quad (13)$$

where A – coefficient, derived from initial conditions.

Thus, considering (10) and (13), the full solution of equation (1) is as follows:

$$\Delta T_r = \frac{\Delta T_{en.m}}{\sqrt{1+\omega_r^2 R_r^2}} sin(\omega_r t - \varphi_r) + Ae^{-t/R_r}. \quad (14)$$

Under initial circumstances, thus $t = 0$, ΔT_r, based on (14), an expression was obtained to determine the coefficient A:

$$A = \frac{\Delta T_{en.m}}{\sqrt{1+\omega_r^2 R_r^2}} sin\,\varphi_r. \quad (15)$$

Expression for immediate values ΔT_r temperature of the massive rotor at a sinusoidal change in the medium temperature in time ΔT_{en} can be presented as follows:

$$\Delta T_r = \frac{\Delta T_{en.m}}{\sqrt{1+\omega_r^2 R_r^2}} \left[sin(\omega_r t - \varphi_r) + e^{-t/R_r} \cdot sin\,\varphi_r\right]. \quad (16)$$

The harmonic composition of current and voltage was determined on an experimental model of an electric screw unit for grinding and pyrolysis of plant waste biomass. Figure 5 shows the electric auger's operating chamber, and Figure 6 shows the wiring diagram for the measuring instruments.

The following measuring instruments were used during the empirical research: Hantek 6254BC four-channel digital USB oscilloscope (manufactured in China); Tenmars TM-191 Magnetic Field Meter (manufactured in Taiwan), designed to measure ultra-low frequency electromagnetic fields from 30 Hz to 300 Hz; Tenmars TM-190 Multi-Field EMF Meter (Taiwan) – a device for measuring high-frequency electromagnetic fields in the frequency range from 50 MHz to 3.5 GHz and low-frequency electric and magnetic fields in the frequency range of 50-60 Hz; infrared, optical pyrometer BENETECH GM533A (China), measuring range – 50-530°C, visibility index 12: 1, thermal radiation coefficient 0.1-1, spectrum 5-14 microns.

Figure 5. Operation chamber of the electric auger unit for shredding and pyrolysis of plant waste biomass (upper part of the housing removed)

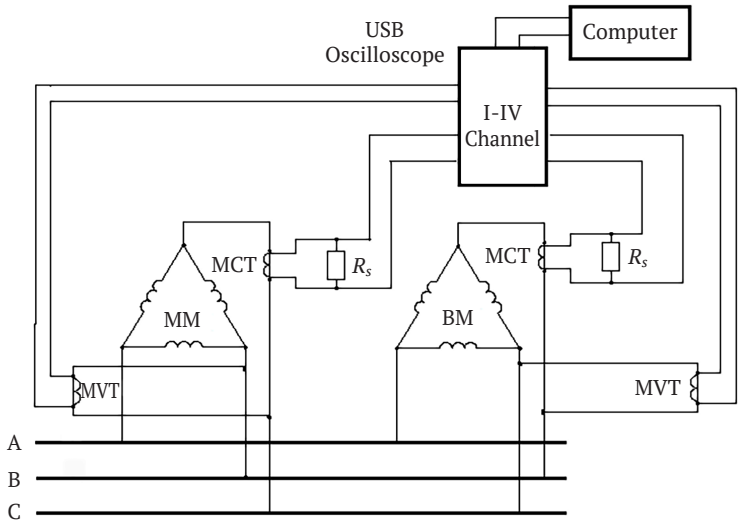

Figure 6. Wiring diagram for measuring devices
Note: MM, BM – stator windings of the motor and brake modules, respectively; MVT, MCT – voltage and current measuring transformers; R_s – shunt; A, B, C – electricity network phases
Source: compiled by the authors

To understand in detail the complete picture of the temperature and magnetic fields in the screw electromechanical hydrolyser and the unit for pyrolysis of biomass from plant waste, mathematical modelling (MM) was carried out using the finite element method in the Comsol Multiphysics software environment. The electromagnetic field was analysed based on Maxwell's system of equations. To determine the current density induced in the rotor, the following expression can be used, which follows from the first equation of Maxwell's system of equations:

$$J_z = rot_z H = \frac{1}{\mu}\left(\frac{\partial B_y}{\partial x} - \frac{\partial B_x}{\partial y}\right). \quad (17)$$

The differential equation of the thermal field in partial derivatives concerning temperature T is as follows:

$$\Delta T - c\rho\frac{\partial T}{\partial t} = -Q, \quad (18)$$

where λ, c, ρ – respectively thermal conductivity, heat capacity and density of the material; Q – specific heat loss.

At each point of the rotor, the specific losses are calculated using the following expression:

$$Q = J_z^2/\gamma(T), \quad (19)$$

where the electrical conductivity of the rotor iron at each point depends on the temperature T.

In Cartesian coordinates for a two-dimensional field picture, equation (18) is rewritten as follows:

$$\lambda\frac{\partial^2 T}{\partial x^2} + \lambda\frac{\partial^2 T}{\partial y^2} - c\rho\frac{\partial T}{\partial t} = Q. \quad (20)$$

The interrelation of the equations of the electromagnetic and thermal fields is manifested in the mutual influence of temperature, electrical conductivity, eddy current density, and specific heat losses, which is reflected in expressions (17-19). Boundary and initial conditions are set for equation (20). The choice of boundary conditions is determined by the peculiarities of the operating modes. The most favourable conditions for the process of generating higher harmonics were chosen for the study – the mode of gradual filling of the screw, and for comparison – the mode of a single-mass system at idle stroke. In this case, when constructing the MM, we assume that the main heat transfer from the rotor to its upper part is carried out by convective heat exchange between the heated surface and the airflow (area G_2, Fig. 3) Such heat transfer occurs following the Newton-Richman law, and a boundary condition of the third kind is set at the corresponding boundary:

$$\left.\frac{\partial T}{\partial n}\right|_{G_1,G_2} = -\frac{\alpha}{\lambda}(T - T_0), \quad (21)$$

where α – heat dissipation coefficient; T_0 – coolant air temp.

The boundary condition (21) is also set on the inner surface of the fixed hollow shaft and the surfaces of the axial ventilation channels made in the stator core. The heat transfer on the lower part of the rotor surface (area G_1, Fig. 3) in contact with the transported bulk material has a complex physical nature. From the physical point of view, the most adequate assumption is that the joule losses generated in the lower half of the rotor are transferred to the bulk material in the form of heat flow through the surface G_1. This assumption is met by a boundary condition of the second kind, which sets the average value of the heat flux at the boundary of the computational domain:

$$q|_{G_1'} = \frac{1}{R_{2н}}\int_{S'} Q\, ds = \frac{1}{R_{2н}}\int_{S'}[J_z^2/(\gamma)T]\, ds, \quad (22)$$

where $R_{2н}$ – external rotor radius; S' – integration region. Condition (22) also determines the relationship between the electromagnetic and thermal tasks.

RESULTS AND DISCUSSION

The graphical representation of dependencies (10), (13), and (16) is shown in Figure 7.

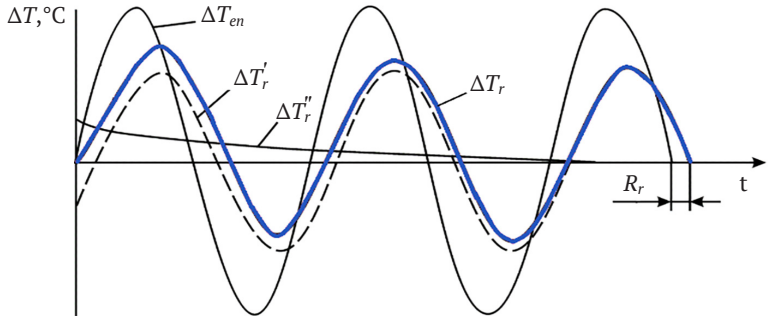

Figure 7. Changes in the rotor temperature of an electromechanical screw converter over time with sinusoidal fluctuations in the medium temperature

Note: R_r – thermal time constant of the rotor design zone; ΔT_r – rotor temp increase; $\Delta T_r'$ – forced rotor temperature increase component; $\Delta T_r''$ – free (aperiodic) component of the rotor temperature increase; ΔT_{en} – increase in ambient temperature

Source: compiled by the authors

As can be seen from the relation (16) and Figure 7, a transient process is observed in the initial time, followed by a sinusoidal change in the rotor temperature, which, in turn, causes pulsations in the specific active resistance ρ and magnetic permeability μ of the rotor material. The influence of temperature on the nature of electromagnetic processes is illustrated by the example of the penetration of an electromagnetic field wave into a massive conductive body. The law of penetration of the induced current deep into the rotor under a harmonically varying magnetic field in time can be approximately expressed by the following expression:

$$J(y) = J_m e^{-ky}, \tag{23}$$

where $k = \sqrt{\omega\mu/2\rho}$; ω – angular frequency of field change; μ – magnetic permeability; ρ – resistivity.

The inverse value$\Delta = 1/k$ is termed the conditional depth of alternating current penetration into the rotor and is equal to the distance from the conductor surface at which the current value decreases by a factor of e. The rotor resistivity is linearly dependent on temperature according to the known law:

$$\rho = \rho_0[1 + \alpha(T - T_0)], \tag{24}$$

where ρ_0 – resistivity at temperature T_0.

The dependence of the magnetic permeability of steel on temperature is more complex and is determined by empirical dependencies. In this study, the structural carbon steels were found to have the following values μ in the strong field range ($H = 2 \cdot 10^{-3}...12 \cdot 10^{-3}$ A/m) have slight fluctuations when heated to temperature 400°C, but then begin to decrease with increasing temperature, reaching unity at the Curie point temperature, which coincides with the data. All other conditions being equal, as the rotor temperature T increases, the depth of penetration of its currents also increases:

$$\Delta = \sqrt{2\rho_0[1 + \alpha(T - T_0)]/\omega\mu}. \tag{25}$$

There is a limited amount of data in the published literature on the effect of temperature and pressure on the magnetic properties of steel, for example, in the case of submersible motors used in oil wells or deep-sea oil-filled motors (Zou *et al.*, 2012; Zhang *et al.*, 2016). It is difficult to determine the magnetic properties of electrical steel sheets in an environment where temperature and pressure are coupled using known data and hysteresis models. Therefore, to improve the accuracy of EM design calculations, it is necessary to know the magnetic properties of steel under the same conditions. Such an analysis was carried out by L. Xiao *et al.* (2019) who found that the relative permeability at low flux densities increases with increasing temperature and decreases at higher flux densities. At the same time, when the compressive stress exceeds 50 MPa, the effect of compressive stress on the relative permeability and iron loss decreases. The relative permeability and iron loss of electrical steel sheets were experimentally determined at conditions from 30°C to 200°C and from 0.1 MPa to 140 MPa. The study by A. Boehm & I. Hahn (2014) and A. Yao *et al.* (2018) measures the magnetic properties of steel and other soft magnetic, electrically conductive materials at high temperatures up to the Curie temperature and above. The measurements show that the saturation polarisation decreases slightly up to 500°C and then drops to zero at temperatures above 700°C. The peculiarity of the considered methods and results of research on electromechanical transducers is the stationary temperature conditions of the surrounding cooling medium. However, for a wide class of multifunctional electromechanical converters for technological purposes, studies with nonlinear changes in the load-cooling medium become relevant.

Transient processes that occur when the rotor temperature fluctuates with changes in ambient temperatures

are accompanied by the appearance of harmonics of currents and rotor magnetomotive force. Figure 8 shows the temperature distribution in the cross-section of an electric screw unit for grinding and pyrolysis of plant waste biomass at a rotor speed of 10 rpm in the mode of gradual filling of the screw, provided that the lower part of the rotor (area G_1, Fig. 3) is immersed in a bulk material. In this zone, endothermic reactions and intensive heat transfer from the rotor to the raw material occur. The upper part of the rotor (area G_2, Fig. 3) is in contact with air, the thermal conductivity of which at temperatures above 250°C is 0.025 W/m·K, which is an order of magnitude less than the thermal conductivity of the raw material being processed. From the presented results, it follows that the temperature difference between the lower and upper parts of the rotor can reach 60-80°C. The stator winding temperature does not reach the maximum permissible values for electrical insulation.

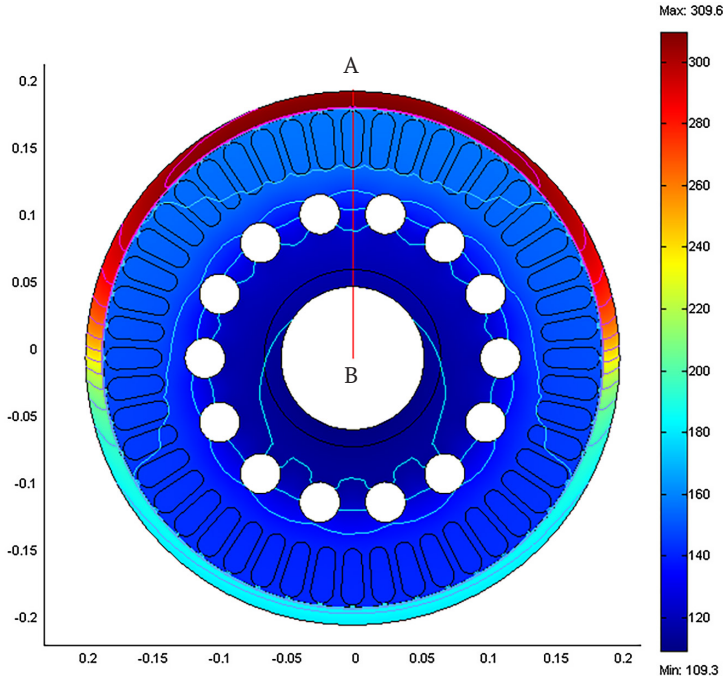

Figure 8. Temperature distribution in the cross-section of an electric screw unit at a rotor speed of 10 rpm in the mode of gradual filling of the screw

Source: compiled by the authors

In the operating zones of the twin-screw electromechanical hydrolyser (Fig. 9), which are located between the rotors, a significant (up to 60) difference in the temperature of the rotors is observed compared to the zones located between the screw and the wall of the reaction chamber.

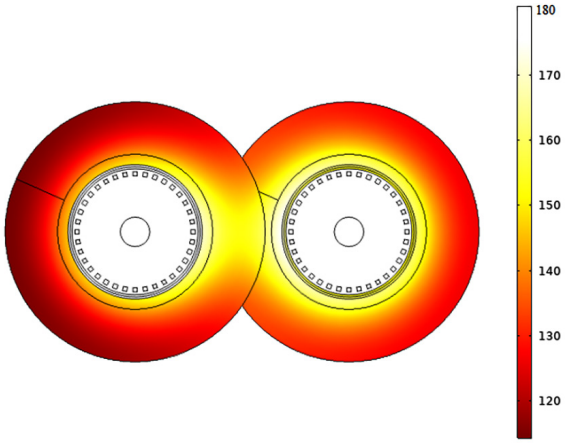

Figure 9. Heating of electromagnetic parts of a twin-screw electromechanical hydrolyser

Source: compiled by the authors

The literature compares different cooling methods, their volumetric flow rates and other machine parameters concerning continuous power for EM designs with both internal and external rotors. M. Vukotić *et al.* (2023) conducted an analysis using experimental testing and computational fluid dynamics modelling to derive a generalised analytical equation for the stator winding calculation related to blade geometry and rotor speed. As the machine size increases, winding cooling becomes less efficient for heat sources in the centre of the machine, while the heat transfer in the cooling jacket increases. R. Lehmann *et al.* (2022) proved that sensitivity studies of other machine parameters, such as the maximum allowable magnet temperature or the coolant inlet temperature (oil or water), improve the understanding of how to increase continuous EM power when rotor temperature limits performance. A. Tovar-Barranco *et al.* (2020) proposed a methodology for obtaining convection heat transfer coefficients for synchronous motor windings using concentrated parameters. However, these publications do not consider models for increasing the efficiency of an electric machine by thermal integration and the use of the dissipative component of energy for the implementation of technological processes in which EM is involved.

Analysing the current spectrograms obtained experimentally (Fig. 10-12), it can be noted that the higher harmonics in the frequency range (0 ... 500 Hz) are less pronounced than in the voltage spectrograms, but still more pronounced at frequencies of 101 Hz, 105 Hz, 145 Hz, 245 Hz, and 375 Hz. In the range from 0 to 50 kHz, the current spectrograms show harmonics of the following frequencies: 1 kHz; 7 kHz; 15 kHz; 17 kHz; 28.5 kHz; 33 kHz; 35 kHz; 43 kHz.

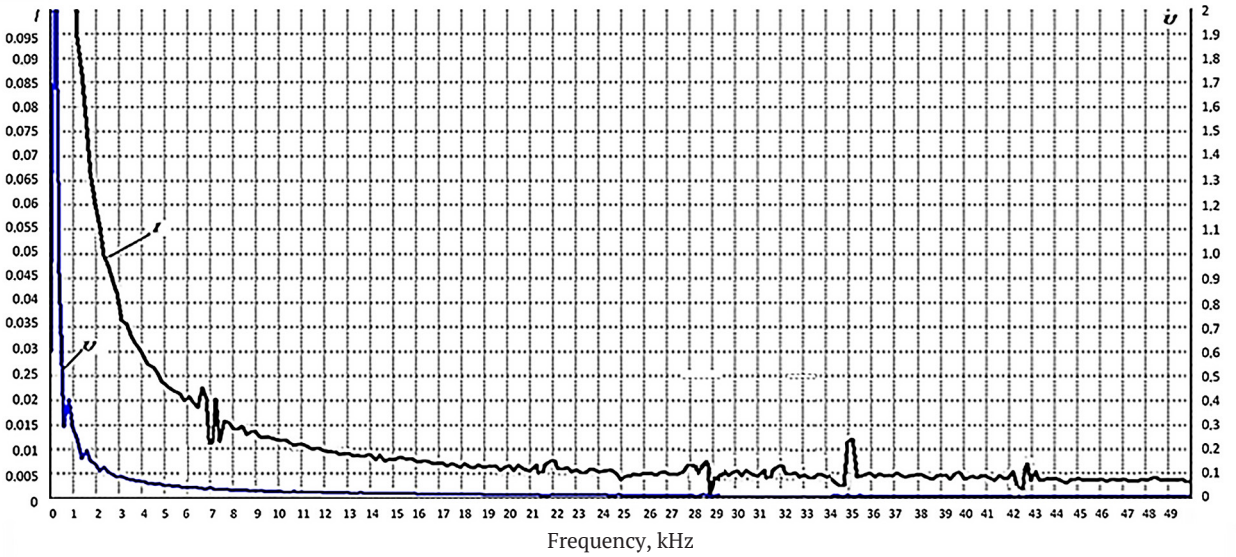

Figure 10. Harmonic composition of current and voltage in the range of up to 50 kHz in the idle mode of the screw
Source: compiled by the authors

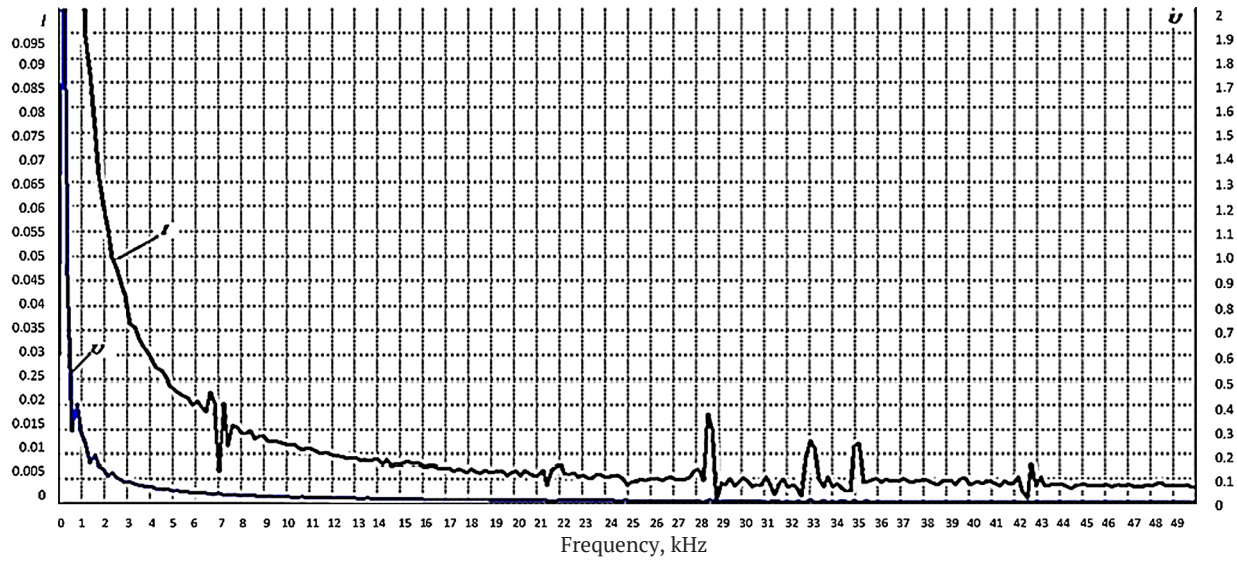

Figure 11. Harmonic current and voltage composition in the range of up to 50 kHz for gradual screw-filling mode
Source: compiled by the authors

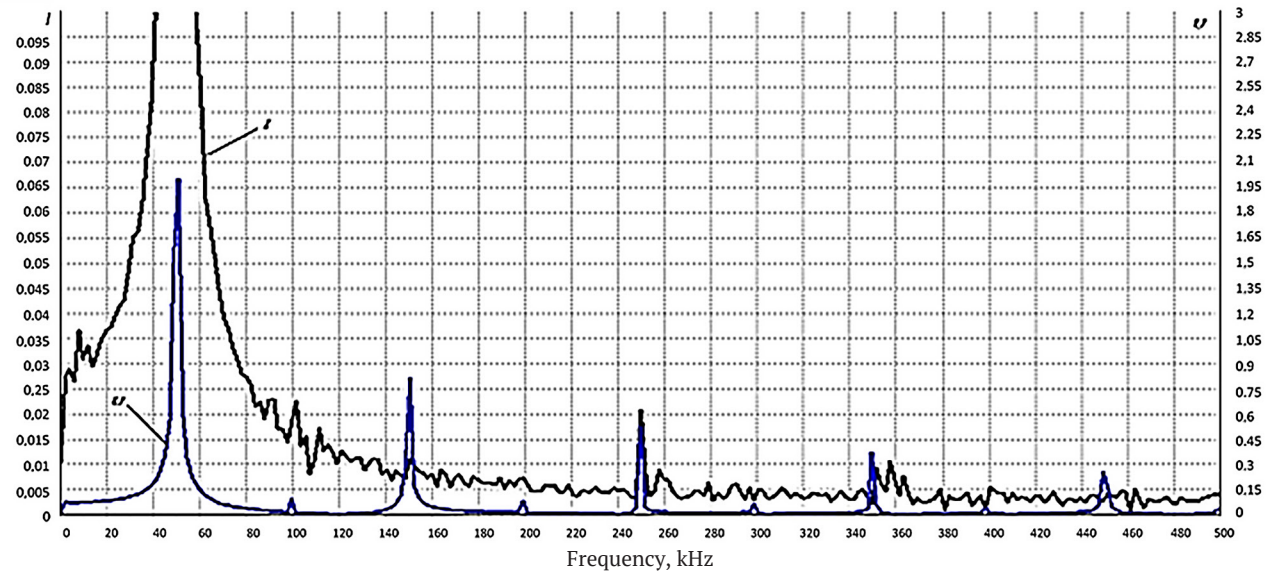

Figure 12. Harmonic current and voltage composition in the range of up to 500 Hz for gradual screw-filling mode
Source: compiled by the authors

In the case of nonlinear temperature changes in the induction machine environment, higher time-dependent harmonics arise, and the magnetic field shape becomes deformed. The highest values of higher harmonic amplitudes occur during thermal shocks. S. Bjelić *et al.* (2011) experimentally registered the appearance of such harmonics, but no theoretical justification for this phenomenon was proposed. A. Funke *et al.* (2018) found the inefficiency of the screw converter in the initial mixing area, which leads to uneven heat transfer under suboptimal conditions. J. Muñoz Tabora *et al.* (2020) conducted a comparative analysis of the effect of harmonic voltages on the performance and temperature rise of IE2, IE3, and IE4 electric motors. The results show that under ideal operating conditions, the permanent magnet motor of class IE4 has better consumption and temperature performance but has nonlinear characteristics. In the presence of voltage harmonics, this scenario completely changes according to the harmonic content. To analyse the effect of harmonics on the motor temperature rise, a statistical analysis using Spearman correlation matrices is presented.

Comparing the current spectrograms in Figure 10 and Figure 11, it is possible to note the difference in amplitudes and the presence of certain harmonics for the idle screw mode and the gradual screw-filling mode. This is especially evident at frequencies of 7 kHz, 28.5 kHz, 33 kHz, and 35 kHz, which confirms the effect of generating higher harmonics when the temperature of the medium surrounding the rotor screw changes. The main factor that influenced the generation of higher harmonics of these frequencies should be considered the presence of a free (aperiodic) component of changes in the temperature of the rotor of the screw electromechanical converter over time with sinusoidal fluctuations in the temperature of the medium.

The modifications of electromechanical converters for technological purposes proposed in this study provide regulation of heat and mass transfer due to the two-way supply of thermal energy to raw materials and the ability to directly influence the technological process through the parameters and characteristics of the electromagnetic system. At the same time, a mathematical model (algorithm) can be introduced to determine the state of the induction machine, as well as a modelling procedure for measuring certain values in MATLAB, which is presented in N. Marković *et al.* (2017). The measurement process in the system is gradually developing and improving as a combination of information and results of previous modelling steps with new elements, for example, when the stator windings of the motor and braking modules of the electromechanical converter are powered by a frequency converter, respectively.

In terms of the physics of thermomagnetic processes, the results of the electric screw machine research are comparable to those of thermomagnetic motors (Hey *et al.*, 2022). A thermomagnetic motor uses a change in the magnetic resistance of a thermomagnetic material to generate a force or torque, in which there is a temperature fluctuation as it rotates. The rate of temperature change in the thermomagnetic material can be estimated from the thermal time constant of the first-order system, similar to Equation (1). Based on the known physical properties and heat transfer parameters, the time constant is also several seconds. According to the research of J. Hey *et al.* (2022), in a thermomagnetic motor, in which temperature fluctuations occur as the rotor rotates at a speed of 11 rpm, fluctuations in force or torque are observed with a frequency of 0.75 Hz. In our studies of the electric screw unit at a rotor speed in the range of 10…45 rpm in the mode of gradual filling of the screw in the harmonic composition of currents (Fig. 12), we also observe frequencies of 0.17…0.75 Hz. However, unlike in the study of J. Hey *et al.* (2022), the appearance of a spectrum of low-frequency

and high-frequency harmonics in an electric screw unit is mainly due not to changes in the magnetic permeability of the magnetic material, but to changes in the rotor resistivity and the depth of current penetration with fluctuations in the rotor temperature.

D. Solomon (1988) suggested a conceptual model of a thermomagnetic generator, stating that the efficiency of a thermomagnetic generator can be increased if the magnetic field is also cyclically changing, as well as the properties of the material to which it is applied. This is the scenario implemented in our electric screw unit in the low-frequency harmonic region.

Among the existing publications, there are many studies devoted to the study of thermal processes occurring in screw converter devices. F. Campuzano *et al.* (2019) studied the effects of heat transfer on the processed material. The heat transfer effect in a twin-screw converter was found to be better than in a single-screw converter. This effect is confirmed in these studies, as well as by M.M. Zablodskiy *et al*. (2022). F. Qi & M.M. Wright (2020) performed mathematical modelling of the processes of hydrodynamics, heat transfer, and chemical reactions of particles in a twin-screw converter. The proposed F. Qi & M.M. Wright's (2020) models in combination with the models of electromagnetic and thermal processes of this work can be considered as a direction for further research, provided that the heat of reaction parameter is carefully calibrated to improve the kinetic model.

An important result of this study is the theoretical and practical confirmation of the existence of an additional spectrum of harmonics arising from sinusoidal fluctuations in the temperature of the load-cooling medium. Based on the possibilities of implementing structural, functional, and thermal integration in the proposed modifications of screw electromechanical converters for technological purposes, the identified spectrum of harmonics participates in the formation of both the dynamics of the rotating system and additional thermal power. This contributes to an increase in the overall efficiency of the screw electromechanical converter.

CONCLUSIONS

The creation of electromechanical converters for technological purposes is based on the idea of combining one electromechanical device simultaneously heating, transporting, magneto-oscillating, mixing functions, integrating thermal energy, and directing the latter to the raw material processing zone. The peculiarity of the considered modifications of the electromechanical converter for technological purposes is that the processed raw material acts as a loading and cooling medium.

The effect of the appearance of the spectrum of higher harmonics in the air gap under nonlinear changes in the temperature of the medium is theoretically substantiated for applications in a twin-screw electromechanical hydrolyser and an electric screw unit for grinding and pyrolysis of biomass of plant waste.

A mathematical model of interconnected electromagnetic and thermal processes is proposed due to the mutual influence of temperature, electrical conductivity, eddy current density, and specific heat losses. Based on the results of numerical modelling, the temperature distribution in the cross-section of the electric screw unit at a rotor speed of 10 rpm in the mode of gradual filling of the screw and the level of heating of the electromagnetic parts of the twin-screw electromechanical hydrolyser were determined.

The appearance of a spectrum of higher harmonics in the range from zero to 50 kHz in an electric screw unit for grinding and pyrolysis of biomass of plant waste has been experimentally recorded. The presence of higher harmonics contributes to an increase in the share of useful thermal energy.

Further research can be devoted to the development of designs and control systems for industrial models of high-temperature screw electromechanical units.

ACKNOWLEDGEMENTS

This work was supported by the Ministry of Education and Science of Ukraine (№0123U102165).

CONFLICT OF INTEREST

The authors declare no conflict of interest.

REFERENCES

[1] Bjelić, S., Marković, N., & Jakšić, U. (2011). The simplified procedure for calculation of the influence of thermal losses on decrease of technical endurance of electric equipment. In *Conference on Industrial Energy and Environmental Protection IEEP'11* (p. 28). Belgrade, Serbia.

[2] Boehm, A., & Hahn, I. (2014) Measurement of magnetic properties of steel at high temperatures. In *40th annual conference of the IEEE industrial electronics society* (pp. 715-721). doi: 10.1109/IECON.2014.7048579.

[3] Campuzano, F., Brown, C.R., & Martínez, J.D. (2019). Auger reactors for pyrolysis of biomass and wastes. *Renewable and Sustainable Energy Reviews*, 102, 372-409. doi: 10.1016/j.rser.2018.12.014.

[4] Elmadah, H., Roger, D., & Takorabet, N. (2019). Design of inorganic coils for high temperature electrical machines. *Open Physics*, 17(1), 698-708. doi.org/10.1515/phys-2019-0072.

[5] Feng, C., Li, Z., Wang, Z., Wang, B., & Wang, Z. (2019). Optimizing torque rheometry parameters for assessing the rheological characteristics and extrusion processability of wood plastic composites. *Journal of Thermoplastic Composite Materials*, 32(1):123-140. doi: 10.1177089270571774482 8.

[6] Funke, A., Grandl, R., Ernst, M., & Dahmen, N. (2018). Modelling and improvement of heat transfer coefficient in auger type reactors for fast pyrolysis application. *Chemical Engineering and Processing – Process Intensification*, 130, 67-75. doi: 10.1016/j.cep.2018.05.023.

[7] Gritsyuk, V., Nevliudov, I., Zablodskiy, M., & Subramanian, P. (2022). Estimation of eddy currents and power losses in the rotor of a screw electrothermomechanical converter for additive manufacturing. *Machinery & Energetics*, 13(2), 41-49. doi: 10.31548/machenergy.13(2).2022.41-49.

[8] Hey, J., Tan, J.L., & Tan, Z.H. (2022). An evaluation of thermomagnetic motors for heat energy harvesting. In *2022 IEEE/ASME International Conference on Advanced Intelligent Mechatronics* (pp. 1347-1354). Sapporo, Japan. doi: 10.1109/AIM52237.2022.9863263.

[9] Juszczak, E.N., Roger, D., Komeza, K., Lefik, M., & Napieralski, P. (2020). Architecture choices for high-temperature synchronous machines. *Open Physics*, 18(1), 683-700. doi: 10.1515/phys-2020-0154.

[10] Laidoudi, A., Duchesne, S., Morganti, F., & Velu, G. (2020). High-power density induction machines with increased windings temperature. *Open Physics*, 18(1), 642-651. doi: 10.1515/phys-2020-0131.

[11] Lefik, M., Komeza, K., Napieralska-Juszczak, E., Roger, D., & Napieralski, P.A. (2019). Comparison of the reluctance laminated and solid rotor synchronous machine operating at high temperatures. *COMPEL-The international journal for computation and mathematics in electrical and electronic engineering*, 38(4), 1111-1119. doi: 10.1108/COMPEL-10-2018-0405.

[12] Lehmann, R., Künzler, M., Moullion, M., & Gauterin, F. (2022). Comparison of commonly used cooling concepts for electrical machines in automotive applications. *Machines*, 10(6), article number 442. doi: 10.3390/machines10060442.

[13] Marković, N., Bjelić, S., Živanić, J., & Jakšić, U. (2017). Simulation of the impact of higher harmonics on the transient process of induction machine fed from PWM inverters. *Tehnički Vjesnik*, 24(1), 265-271. doi: 10.17559/TV-20150502231618.

[14] Mazlan, M.M., Talib, R.A., Mail, N.F., Taip, F.S., Chin, N.L., Sulaiman, R., Shukri, R., & Mohd Nor, M.Z. (2019). Effects of extrusion variables on corn-mango peel extrudates properties, torque and moisture loss. *International Journal of Food Properties*, 22, 54-70. doi: 10.1080/10942912.2019.1568458.

[15] Muñoz Tabora, J., de Lima Tostes, M.E., Ortiz de Matos, E., Mota Soares, T., & Bezerra, U.H. (2020). Voltage harmonic impacts on electric motors: A comparison between IE2, IE3 and IE4 induction motor classes. *Energies*, 13(13), article number 3333. doi: 10.3390/en13133333.

[16] Mushtruk, M., Gudzenko, M., Palamarchuk, I., Vasyliv, V., Slobodyanyuk, N., Kuts, A., Nychyk, O., Salavor, O., & Bober, A. (2020). Mathematical modeling of the oil extrusion process with pre-grinding of raw materials in a twin-screw extruder. *Potravinarstvo Slovak Journal of Food Sciences*, 14, 937-944. doi: 10.5219/1436.

[17] Patent of Ukraine No. 125774 (2022, June). Retrieved from https://sis.ukrpatent.org/uk/search/detail/1690697/.

[18] Qi, F., & Wright, M.M. (2020). A DEM modeling of biomass fast pyrolysis in a double auger reactor. *International Journal of Heat and Mass Transfer*, 150(2), article number 119308. doi: 10.1016/j.ijheatmasstransfer.2020.119308.

[19] Singha, P., & Muthukumarappan, K. (2016). Effects of processing conditions on the system parameters during single screw extrusion of blend containing apple pomace. *Journal of Food Process Engineering*, 40(4), article number e12513. doi: 10.1111/jfpe.12513.

[20] Solomon, D. (1988). Improving the performance of a thermomagnetic generator by cycling the magnetic field. *Journal of Applied Physics*, 63(3), 915-921. doi: 10.1063/1.340033.

[21] Subramanian, R.S. (2014). *Conduction in the cylindrical geometry*. Retrieved from https://web2.clarkson.edu/projects/subramanian/ch330/notes/Conduction%20in%20the%20Cylindrical%20Geometry.pdf.

[22] Tovar-Barranco, A., López-de-Heredia, A., Villar, I., & Briz, F. (2020). Modeling of end-space convection heat-transfer for internal and external rotor PMSMs with fractional-slot concentrated windings. *IEEE Transactions on Industrial Electronics*, 68(3), 1928-1937. doi: 10.1109/TIE.2020.2972471.

[23] Vukotić, M., Lutovski, S., Šutar, N., Miljavec, D., & Čorović, S. (2023). Thermal effects in the end-winding region of electrical machines. *Energies*, 16(2), article number 930. doi: 10.3390/en16020930.

[24] Xiao, L., Yu, G., Zou, J., Xu, Y., & Liang, W. (2019). Experimental analysis of magnetic properties of electrical steel sheets under temperature and pressure coupling environment. *Journal of Magnetism and Magnetic Materials*, 475, 282-289. doi: 10.1016/j.jmmm.2018.11.107.

[25] Yao, A., Odawara, S., & Fujisaki, K. (2018). Iron loss and hysteretic properties under PWM inverter excitation at high ambient temperatures. *IEEJ Journal of Industry Applications*, 7(4), 298-304. doi: 10.1541/ieejjia.7.298.

[26] Zablodskiy, M., Zhyltsov, A., Nalyvaiko, V., Trokhaniak, V., Pugalendhi, S., & Subramanian, P. (2020). Biomass pyrolysis using a multifunctional electromechanical converter and a magnetic field. *Scientia Agriculturae Bohemica*, 51(2), 65-73. doi: 10.2478/sab-2020-0009.

[27] Zablodskiy, M.M., Kovalchuk, S.I., Pliuhin, V.E., & Tietieriev, V.O. (2022). Indirect field-oriented control of twin-screw electromechanical hydrolyzer. *Electrical Engineering & Electromechanics*, 1, 3-11. doi: 10.20998/2074-272X.2022.1.01.

[28] Zhang, S.B., Zheng, X.W., Feng, L.J., Wang, Y.F., & Liu, Z.F. (2016). The design and experimental research of cooling structure in deep well submersible motor. *Journal of Discrete Mathematical Sciences and Cryptography*, 19(3), 837-848. doi: 10.1080/09720529.2016.1197571.

[29] Zou, J., Qi, W., Xu, Y., Xu, F., Li, Y., & Li, J. (2012). Design of deep sea oil-filled brushless DC motors considering the high pressure effect. *IEEE Transactions on Magnetics*, 48(11), 4220-4223. doi: 10.1109/TMAG.2012.2204731.

Кшиштоф Мудрик
Професор
Університет сільського господарства в Кракові
30-149, пр. Адама Міцкевича, 21, м. Краків, Польща
https://orcid.org/0000-0002-6212-6958

Тарас Гуцол
Професор
Університет сільського господарства в Кракові
30-149, пр. Адама Міцкевича, 21, м. Краків, Польща
https://orcid.org/0000-0002-9086-3672

Микола Миколайович Заблодський
Доктор технічних наук, професор
Національний університет біоресурсів і природокористування України
03041, вул. Героїв Оборони, 15, м. Київ, Україна
https://orcid.org/0000-0001-8889-8158

Дмитро Сергійович Сорокін
Кандидат технічних наук, доцент
Національний університет біоресурсів і природокористування України
03041, вул. Героїв Оборони, 15, м. Київ, Україна
https://orcid.org/0000-0002-1762-9724

Сергій Миколайович Усенко
Кандидат технічних наук, доцент
Національний університет біоресурсів і природокористування України
03041, вул. Героїв Оборони, 15, м. Київ, Україна
https://orcid.org/0000-0001-7225-9589

Дослідження електротепломеханічного перетворювача технологічного призначення при нелінійних змінах навантажувально-охолоджуючого середовища

Анотація. У сучасному екологічному контексті актуальною стає необхідність оптимізувати технологічні процеси з важкими температурними навантаженнями, забезпечуючи високу надійність і об'єднуючи обертові частини електричних машин з виконавчими механізмами, з метою досягнення більшої ефективності електромеханічних перетворювачів. Метою дослідження було теоретичне обґрунтування та експериментальне підтвердження ефекту появи вищих гармонік в повітряному зазорі при нелінійній зміні температури середовища. Дослідження ґрунтуються на основних положеннях електродинаміки, тепломасообміну, математичного моделювання методом скінченних елементів і експериментальній перевірці мультифізичних параметрів. На основі аналізу диференціального рівняння для визначення приросту температури поверхні феромагнітного ротора в умовах нелінійної зміни температури середовища, що оточує електромеханічний перетворювач, встановлені закономірності формування вільної і вимушеної складової миттєвих значень температури массивного ротора. В залежності від режиму взаємодії навантажувально-охолоджуючого середовища і електромеханічної частини шнекових агрегатів сформовані кінематичні схеми одномасової та двомасових систем зі змінними або постійними моментами інерції та жорсткістю. Згідно розмірів електромагнітної системи експериментального зразка побудована математична модель для досліджень теплових і електромагнітних процесів. Визначено закономірності просторового розподілу температури шнекового електромеханічного агрегата. Експериментально встановлені спектри вищих гармонік напруги та струму в діапазоні частот від 0 до 50 кГц, що підтверджує наявність ефекту генерування вищих гармонік при зміні температури середовища, що оточує ротор-шнек. Виявлений спектр гармонік впливає як на формування динаміки обертової системи, так і додаткової теплової потужності, підвищуючи при цьому загальний коефіцієнт корисної дії шнекового електротепломеханічного перетворювача. Практична цінність отриманих результатів полягає в можливості прогнозування оптимальних показників взаємопов'язаних електромагнітних і теплообмінних процесів в шнекових електромеханічних перетворювачах технологічного призначення

Ключові слова: спектр вищих гармонік; феромагнітний порожнистий ротор; біомаса; температурне поле; електромагнітне поле; конструктивно-технологічна схема